THE AMERICAN SOCIETY OF MECHANICAL ENGINEERS
345 E. 47 St., New York, N.Y. 10017

90-GT-78

Gas Turbine Rotor Blade Film Cooling With and Without Simulated NGV Shock Waves and Wakes

M. J. RIGBY
Rolls-Royce plc,
Derby, U.K.

A. B. JOHNSON
Schlumberger Cambridge Research
Cambridge, U.K.

M. L. G. OLDFIELD
Oxford University,
Oxford, U.K.

ABSTRACT

Detailed heat transfer measurements have been made around a film-cooled transonic gas turbine rotor blade in the Oxford Isentropic Light Piston Tunnel. Film cooling behaviour for four film cooling configurations has been analysed for a range of blowing rates both without and with simulated nozzle guide vane (NGV) shock wave and wake passing. The superposition model of film cooling has been employed in analysis of time-mean heat transfer data, while time resolved unsteady heat transfer measurements have been analysed to determine interaction between film-cooling and unsteady shock wave and wake passing. It is found that there is a significant change of film-cooling behaviour on the suction surface when simulated NGV unsteady effects are introduced.

NOMENCLATURE

A	film-cooling mixing factor
B	film-cooling temperature gain factor
B.R.	blowing rate B.R.= $(\rho U)_c / (\rho U)_g$
C_{TN}	blade chord
D	film-cooling hole diameter
k	thermal conductivity
K	acceleration parameter $K = (\nu/U^2).\ \partial U/\partial x$
L	length, blade surface length from LE to TE
Nu	Nusselt number $Nu = \dot{q}\ C_{TN}/[k(T_g - T_w)]$
NGV	nozzle guide vane
$\dot{q}$	heat transfer rate
T	temperature
T_c	coolant total temperature
T_g	gas recovery temperature
T_w	wall temperature
U	velocity

Greek Symbols

η_{aw}	adiabatic wall film-cooling effectiveness $\eta_{aw} = (-B/A)$
ρ	density
Θ	dimensionless temperature $\left(\frac{T_g - T_c}{T_g - T_w}\right)$

INTRODUCTION

The use of film-cooling on gas turbine rotor blades and vanes is becoming ever more important as turbine entry temperatures move higher, in an attempt to increase thrust and lower specific fuel consumption. Consequently, much research and development effort has been invested to understand and predict the performance of a film-cooling row.

Past research has shown that the performance of a film-cooling row is very sensitive to conditions such as hole shape, blowing rate, pitch/diameter ratio and freestream conditions. In investigating the behaviour of a film-cooling row it is important to correctly simulate the engine environment. The non-dimensional parameters of Reynolds Number, Mach Number, gas-to-coolant density ratio, and gas-to-wall temperature ratio can be modelled in a suitable wind tunnel, while hole configuration, acceleration parameter and surface curvature are functions of the blade profile under test. However, the true flow in a gas turbine is unsteady, and these unsteady effects will be of importance, even though they have, up to now, been generally neglected by the film-cooling designer.

This paper presents film-cooling results for the pressure surface and suction surface of a two-dimensional representation of a gas turbine rotor blade. Measurements in the film-cooled region made without and with simulated nozzle guide vane (NGV) shock waves and wakes show a marked change in film-cooling behaviour.

*Presented at the Gas Turbine and Aeroengine Congress and Exposition—June 11-14, 1990—Brussels, Belgium

EXPERIMENTAL APPARATUS

Heat transfer measurements using platinum thin film gauges painted at the mid-span of a transonic gas turbine blade profile were made in the Oxford University Isentropic Light Piston Cascade Tunnel. This blade has been used in studies by Johnson et al (1988,1989,1990) and Rigby et al (1989). The tunnel has been extensively documented (Jones et al (1973), Schultz et al (1977)). The facility is well suited to the transient heat transfer measurement technique, producing uniform flow conditions over the cascade for about 300ms. The tunnel working section is shown in Figure 1. The upstream turbulence level of approximately 3% was generated by a turbulence grid (2mm diameter bars pitched 15mm apart) located about five blade chords (207mm) upstream of the central blade leading edge.

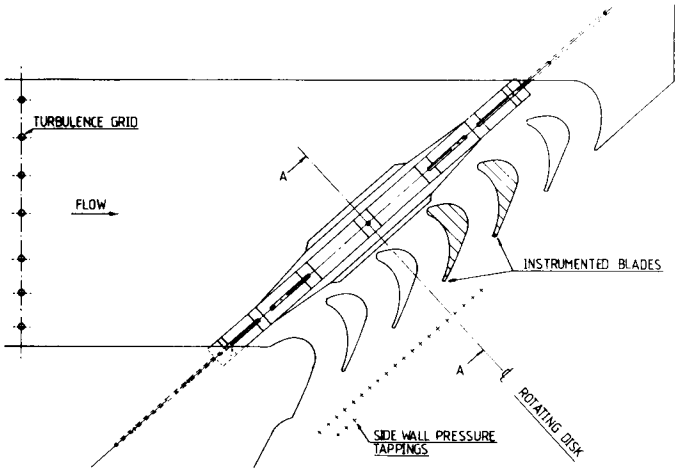

Fig. 1 ILPT Working Section and Instrumented Passage

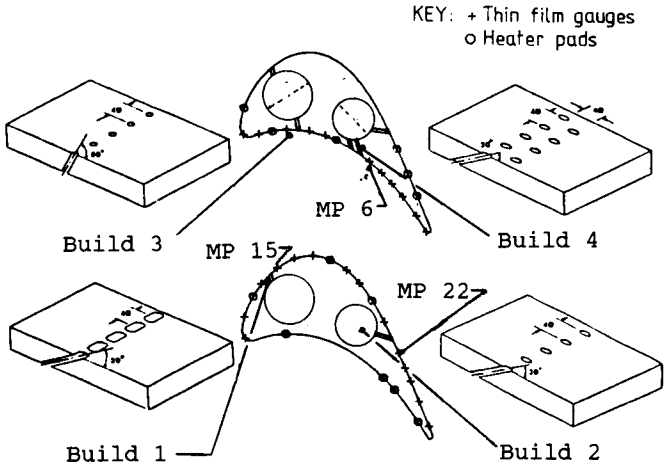

Fig. 2 Cooling Configurations and Instrumentataion Showing Model Points

Figure 2 shows the location of the thin film gauges in the instrumented passage and the four film cooling configurations used. The choice of cooling configuration is discussed in more detail later. Surface heat transfer rate data were obtained directly from the surface temperature measurements using high frequency analogues, as described by Oldfield et al (1984). Two sampling rates were used to record the heat transfer measurements. Mean heat transfer data were recorded by a PDP11/34 mini-computer at 2.5ms sampling intervals for 0.5s. In addition, to resolve the unsteady effects of simulated shock waves and wakes on the heat transfer, part of the run was sampled at a high rate using a Datalab DL2800 series transient recorder, taking 16 channels of 3500 data points per channel at 2μs sampling intervals. Table 1 lists the tunnel conditions used on these tests.

Table 1 Experimental flow conditions

Inlet Mach number	0.38
Exit Mach number	1.18
Bar relative Mach Number	1.13
Reynolds number (based on blade true chord and isentropic exit conditions)	1.0×10^6
Blade chord C_{TN}	41 mm
Blade axial chord	34 mm
Inlet angle	48°
Flow Total temperature	460 K
Inlet total pressure	290 kPa
Bar generator rotational speed	21,800 rpm

Simulation of Shock Wave and Wake Passing

It is important to examine the effect of engine simulation shock wave and wake passing on the blade heat transfer. Moving shock waves and wakes, which would be present in an engine due to the presence of an NGV ring upstream of the moving rotor, were simulated using a 'rotating bar' shock and wake generator, previously described by Doorly et al (1985) and Johnson et al (1988). A set of 148mm long, 1.6mm diameter bars were mounted on a 300mm diameter disc to pass through a plane 14.7mm axially upstream of the cascade leading edge, as shown in Figure 1. In order to simulate engine shock wave and wake passing, the disc was spun with 16 bars attached. A more detailed study of the isolated effects of each shock wave and wake passing was made by using only 2 bars attached to the disc. Engine condition velocity triangles were achieved in both cases at a rotational speed of 21,800 rpm.

As well as the trailing edge wake, each bar will produce two shock waves; a bow shock will stand off the front of the bar and a recompression shock will be formed just downstream of the bar. Only the recompression shock would actually be present in the engine, but, using the time resolved heat transfer measurements, the various components shed from the bar can be identified and their effects separated.

To help understand the heat transfer results and also to track the movement of the events through the passage, a double-pass schlieren system was used. For each condition, five schlieren photographs were taken at different positions in the bar passing sequence. Thus, a comprehensive picture of the movement of the wake

through the passage and the motion of the shock waves could be constructed. By carefully comparing the schlieren results with the time resolved heat transfer traces, it was possible to identify the causes of the observed large excursions in the unsteady heat transfer rate.

The effect of bar passing on the surface heat transfer rates in the vicinity of Build 1 injection can be seen by examination of the unsteady traces shown in Figs. 9 and 10. Figure 10 is a trace obtained with 16 bars in the rotating disk (engine simulated conditions), while Figure 9 is that produced with 2 bars in the disk in order to isolate separate bar passing events. Briefly, there is a rise in heat transfer associated with the bar bow shock. This is followed by a drop in surface heat transfer, which may go negative, due to the expansion fan between the bow shock and recompression shock. The recompression shock then produces another, greater, enhancement in the surface heat transfer rates. The theory to explain the mechanism of heat transfer enhancement associated with shock wave impingement is given in detail by Johnson et al (1988) and Rigby et al (1989). The wake convects over this region after the passage of the shock waves. This will also enhance the surface heat transfer rates due to increased turbulence, although the effect is lost in Figs. 10 and 9 within the heat transfer fluctuations resulting from the shock activity.

Distributions of heat transfer rate were obtained for different gas to wall temperature ratios by keeping the gas and coolant temperatures constant and raising the wall temperature. Heater pads, the locations of which are shown in Figure 2, were painted around the blade surface. During the heating process, the temperature distribution around the blade was monitored via the thin film resistance thermometers, and the current to each heater pad independently controlled to produce a near isothermal wall. The variation in wall temperature during a typical run was of order $\pm$ 6K in approximately 320K.

DATA REDUCTION AND ANALYSIS

The non-dimensional parameter chosen to scale the surface heat transfer measurement was the Nusselt number, defined as

$$Nu = \frac{\dot{q}\, C_{TN}}{k\,(T_g - T_w)} \qquad (1)$$

Choice of this parameter permits the use of the superposition model of film cooling in the analysis of the data. This model (Jones(1982), Choe et al (1974), Teekaram (1989)) is applicable to isothermal wall film-cooling evaluation and uses two constants, A and B, to characterise the film behaviour. The heat transfer rate, q can be written as:

$$\dot{q} = \alpha\,(T_g - T_w) + \beta\,(T_g - T_c) \qquad (2)$$

Rearranging and dividing through by the gas conductivity, k, gives the Nusselt number

$$Nu = A + B\Theta \qquad (3)$$

where

$$\Theta = \frac{T_g - T_c}{T_g - T_w} \qquad (4)$$

A is known as the mixing factor and quantifies the disturbance effect of the film being injected into the boundary layer. B quantifies the cooling performance brought about as a result of the coolant temperature being lower than the gas temperature. This is known as the temperature gain factor and is typically negative. The values of A and B are obtained from the plot of Nu against Θ. It should be noted that this model holds for both positive and negative heat transfer and for $T_g < T_c$ as well as $T_g > T_c$. It would be useful to normalise A and B by dividing through by the unblown Nusselt number, Nu_o at the same conditions. Unfortunately this was not possible for these experiments as the unblown tests were taken on a plain blade, and the boundary layer was not tripped at the film locations.

For zero heat transfer,

$$-B/A = \frac{T_g - T_w}{T_g - T_c} \qquad (5)$$

The parameter $\eta_{aw} = -B/A$ is a form of film cooling effectiveness known as the *isothermal adiabatic wall film cooling effectiveness*. The superposition model has been used by many workers in investigating film cooling, and a thorough description of the technique can be found in several publications (for example Horton(1985) or Teekaram(1989).

In varying Θ it is necessary to maintain a constant value of the ratio T_g/T_c as this defines the physical interaction between the two streams. Altering Θ in this case was achieved by repeating tests with only the wall temperature changed. Collapse of the Nusselt number upstream of the film cooling rows was expected for the range of gas-to-wall temperature ratio employed. However, it was found that some corrections were necessary to the data before achieving the desired collapse. A consistent Nusselt number was required upstream of film-cooling to be certain that variations measured in A and B were due only to the film itself. The corrections applied were for (i)recovery temperature effects; (ii) the presence of the heater pads - these were used to heat the wall, but left a temperature discontinuity at the wall; and finally (iii) for small run to run variations. A more detailed description of the data reduction applied here can be found in Rigby et al(1989).

Application of the Superposition Model

The superposition model has been applied to all of the data reported here. Superposition relies on the enthalpy equation being linear and the uncoupling of the temperature and momentum equations. For the purposes of this study it can be assumed that this is true for both wake passing and no wake passing. However this assumption is not true for regions of the blade affected by shock waves (see Rigby et al (1989)), so the superposition model has not been applied to that region of the blade where significant shock wave activity occurs.

FILM COOLING CONFIGURATIONS

Four film cooling configurations were chosen for this investigation. These are shown schematically in Figure 2. Figure 3 shows the measured Mach number distribution around the blade with film locations marked. The configurations have been chosen to examine the effects of wake and shock wave passing on four distinctly different areas of the blade surface.

Film row 1 lies at 20% suction surface length in a region of strong NGV shock wave activity and wake passing. The blade curvature is moderately convex and the freestream acceleration parameter is 2 x 10^6. Film row 2 is located on the suction surface at 70% surface length. At this location shock wave activity is weak but the wake is still being convected along the surface. The acceleration parameter and local curvature is approximately zero. Film rows 3 and 4 are both on the pressure surface. Row 3 is located at 25% surface length with an angle to surface of 60°. The levels of freestream Mach number and acceleration are low and the surface is concave. Row 4 is a double row of holes at 50% surface length with a nominal angle to surface of 30°. The freestream Mach number in this region is still relatively low, while the acceleration parameter is high at 2.8 x 10^6.

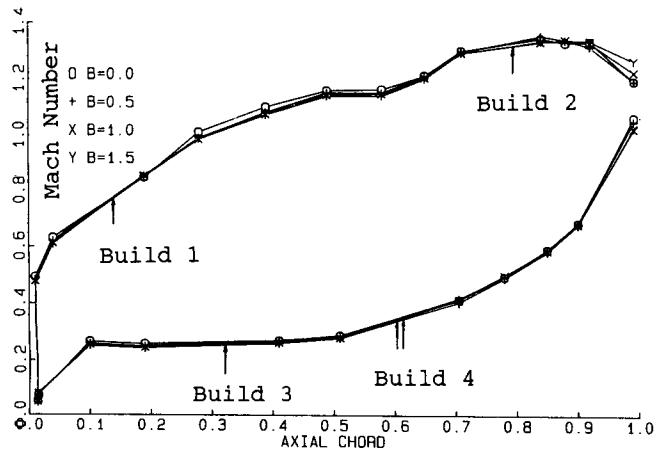

Fig. 3 Measured Mach Number Distribution

DISCUSSION OF FILM COOLING RESULTS

The four film cooling configurations (or builds) tested will be discussed individually, both in terms of the steady state performance and the unsteady behaviour of the film response when disturbed by shock waves and wakes.

The film cooling results on this profile appeared, at first, to be very disappointing. Qualitatively, there was little or no film cooling effect on the pressure surface (see Figure 4) for any of the conditions tested, while ejecting coolant from the double row of holes at 50% pressure surface length enhanced, rather than decreased the downstream heat transfer levels (Fig. 5). A similar result was found by Horton (1985) on the pressure surface of a different profile at high blowing rates. There appeared to be a small cooling effect on the late suction surface (Fig. 5), but not as marked as had been found on other turbine blade profiles, for example Horton (1985).

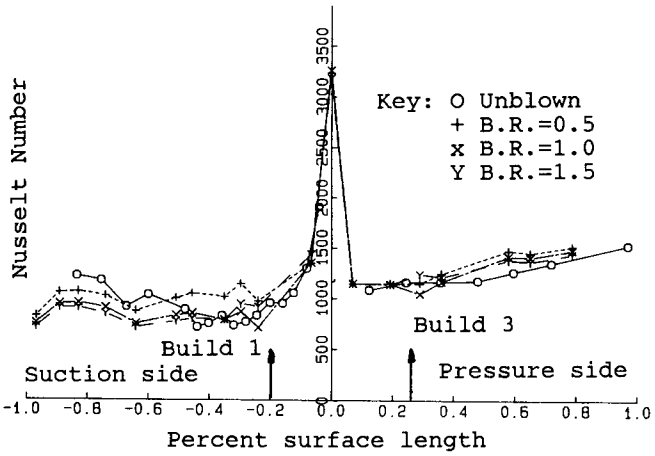

Fig. 4 Mean Nusselt Number for 3 Blowing Rates and Unblown Blade. Zero Bar Passing

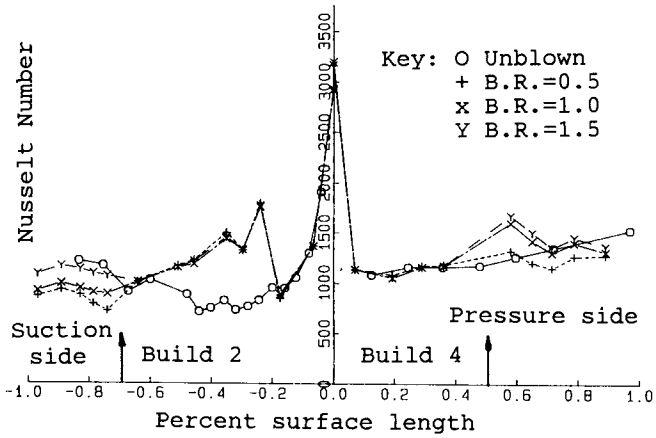

Fig. 5 Mean Nusselt Number for 3 Blowing Rates and Unblown Blade. Zero Bar Passing

Front Suction Surface (Build 1)

The freestream conditions present at this location would suggest a relatively good film-cooling performance from this row. The pressure gradient should hold the coolant onto the blade surface, and lateral mixing would be diminished. The fan-shaped holes will increase the spanwise coverage of the film. However, Figure 4 shows a poor cooling performance from this row. The cooling is improved slightly from B.R.=0.5 to B.R.=1.0, but degrades at a blowing rate of 1.5. This is in contrast with results obtained under similar conditions by other workers, although it agrees with results found by Dunn and Chupp (1987).

Schlieren photographs were taken to examine the trajectory of the coolant for three blowing rates. They indicate that lift-off occurs between B.R.=1.0 and B.R.=1.5. Analysis of the results using superposition support this. Fig. 6 shows A, B and η_{aw} for this build. It can be seen that A increases from B.R.=0.5 to B.R.=1.0 but then falls for B.R.=1.5. This is consistent with an increased disturbance of the boundary layer with blowing rate, while the level of disturbance then falls when lift-off occurs and the film passes through the boundary layer into the freestream. The modulus of B is greater for B.R.=1.0 than

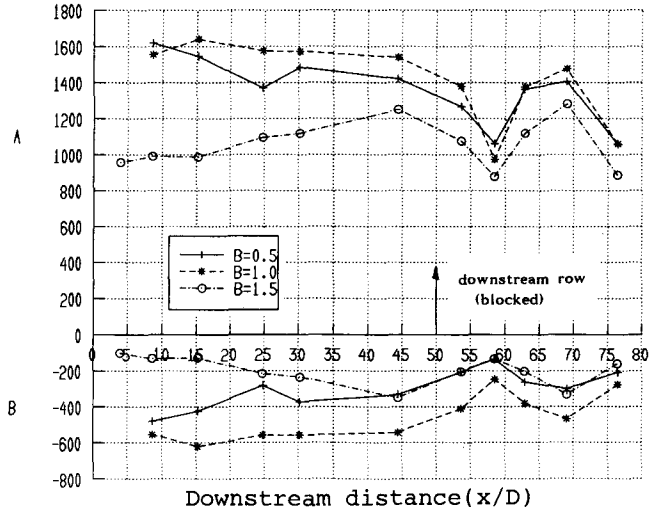

Fig. 6(a) A and B values for Build 1 at 3 blowing rates.

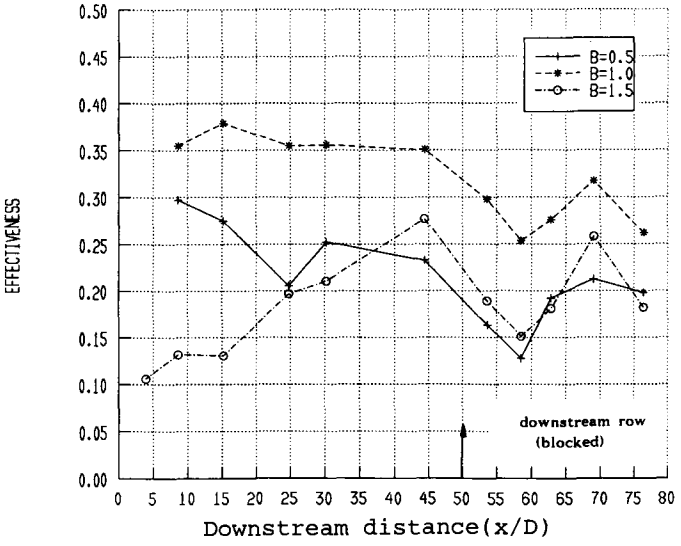

Fig. 6(b) Cooling effectiveness for Build 1 with no bar passing, at 3 blowing rates.

B.R.=0.5 as would be expected from the greater mass flow. Close to the holes however, the value of *B* for a blowing rate of 1.5 is very small - again suggesting that the film is simply passing through the boundary layer. The film then becomes entrained in the boundary layer due to the favourable pressure gradient and a cooling effect is seen further downstream. There is a uniform reduction in *B* following the injection with some oscillation in level around the blocked build 2 row downstream. Even though the holes for build 2 were blocked during the build 1 testing, it appears that they were still able to disturb the boundary layer. This is reflected in the effectiveness levels which do not shown a monotonic decrease with distance downstream.

The effect of bar passing on the surface heat transfer rates in the vicinity of the Build 1 injection can be seen in Figure 7 which shows the mean heat transfer results for this build both with and without injection. Qualitatively,

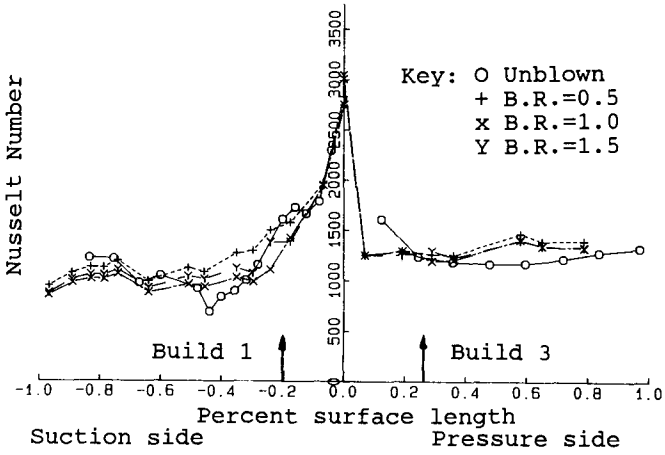

Fig. 7 Mean Nusselt Number for 3 Blowing Rates and Unblown Blade. 16 Bar Passing

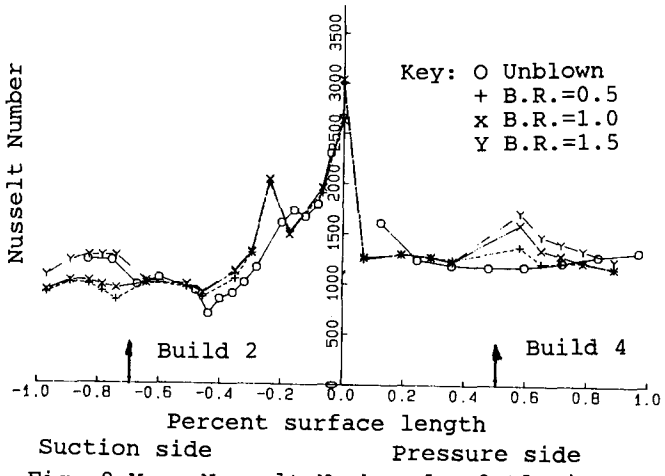

Fig. 8 Mean Nusselt Number for 3 Blowing Rates and Unblown Blade. 16 Bar Passing

the mean heat transfer results show the same effect of film coolant injection for the case of 16 bar passing as for no bar passing. That is, improved cooling performance from B.R.=0.5 to B.R.=1.0 followed by a decrease from B.R.=1.0 to B.R.=1.5. The zero injection case was a plain blade with no blocked holes or boundary layer trips at the injection locations. For a blowing rate of 0.5 there is no cooling effect visible immediately downstream of the film row. Further downstream the case with injection produces higher heat transfer rates than that with no injection. This contrasts with the no bar case but it is dangerous to draw firm conclusions from this due to tripping of the boundary layer by the row of holes.

Quantitative analysis using the superposition theory is not possible here due to the shock wave effects. However, comparison of the mean and unsteady results for the two cases of injection and no injection in this region does reveal some differences. Fig. 9 shows a single cycle, ensemble averaged, for MP15, just downstream of the film row. The figure compares results for no injection, and injection with a blowing rate of 1.5. The reduction in Nusselt number level with film cooling present applies across the full cycle including that part under the influence of the shock waves. Note that the negative

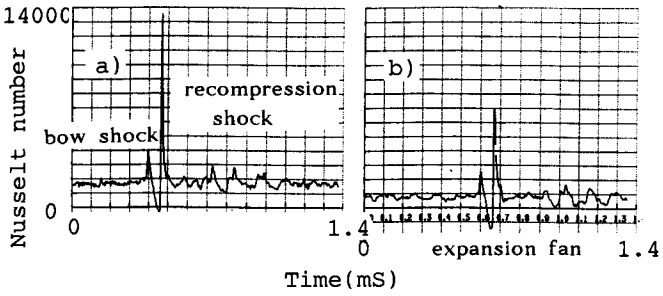

Fig. 9 Unsteady Nusselt number traces at model point 15: a) with no film cooling; b) with cooling at B.R.=1.5. 2 bars in rotating disk.

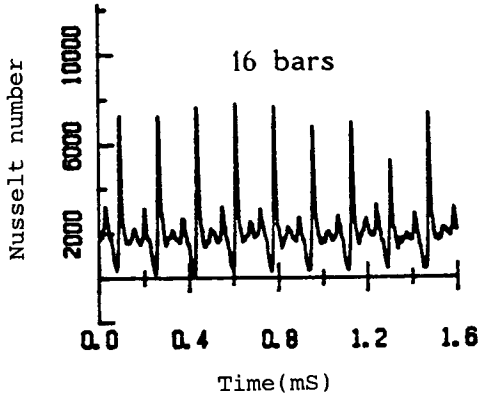

Fig. 10 Unsteady Nusselt number trace at model point 15 for 16 bar passing.

Nusselt number trough due to the expansion fan has also become more negative when film-cooling is present.

Rear Suction Surface (Build 2)

Fig. 5 shows the cooling characteristic of this row in the absence of bar passing plotted for three blowing rates along the blade surface. There is some cooling effect for blowing rates of 0.5 and 1.0, although lift-off is again suggested for a blowing rate of 1.5. When bar passing is introduced the story changes slightly (Fig. 8). Cooling performance is observed for blowing rates of 0.5 and 1.0, but, unlike the case for no bar passing, there is heat transfer enhancement at a blowing rate of 1.5. This result would indicate a greater tendency for the film to lift-off from the blade surface when wake passing is present. This might be an effect of the wake (there is negligible shock wave activity at this point on the blade). The fluid within the wake has lower momentum than that outside, and so the effective blowing rate of the film with wake passing will be marginally higher than that measured. This difference between the steady and unsteady blowing rates could be enough to remove the film-cooling effect of this row. Another effect is the higher level of turbulence within the wake which will increase the mixing of the film and the freestream.

Fig 11 shows η_{aw} for three blowing rates tested at a gas-to-coolant temperature ratio of 1.6, showing a general decrease in effectiveness level as the film mixes downstream. The low level of effectiveness for B.R.=1.5 indicates that the film is lost in the freestream. The lower

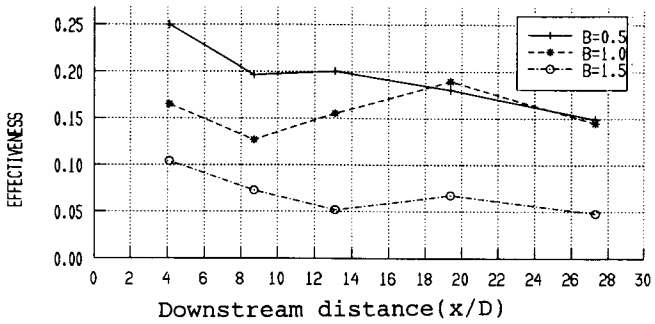

Fig. 11 Cooling effectiveness for Build 2 with no bar passing, at 3 blowing rates.

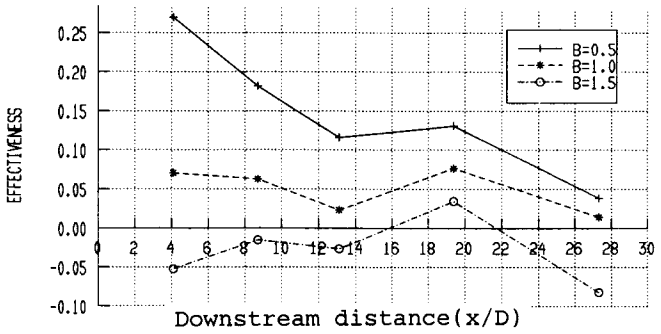

Fig. 12 Cooling effectiveness for Build 2 with 16 bar passing, at 3 blowing rates.

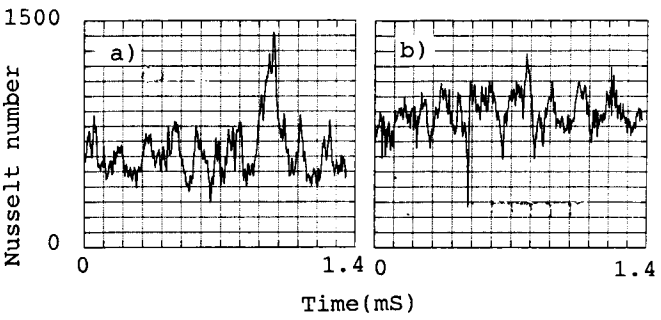

Fig. 13 Unsteady Nusselt number traces at model point 22: a) with no film cooling; b) with cooling at B.R.=1.5. 2 bars in rotating disk.

result for B.R.=1.0 than B.R.=0.5 also suggests that a proportion of the film is lost in the freestream.

The effectiveness results indicate a poorer cooling performance when bar passing is present than without (Fig. 12). The effectiveness level for B.R.=0.5 for the 16 bar case starts at a similar level to the no bar passing case, but falls more rapidly to zero. The greater decay rate of effectiveness with bar passing is probably due to increased mixing between the coolant and the freestream. The values of effectiveness for B.R.=1.0 and 1.5 are lower for the wake passing case, the result for B.R.=1.5 being essentially zero within experimental error. This again suggests a greater level of lift-off of the film with wakes than without.

The effect of film cooling on the unsteady heat transfer traces can be seen in Figures 13(a) and (b) for MP22. Figure 13(a) is the trace for the case of no film-cooling. Here the wake can be seen to produce a significant change in the unsteady heat transfer level, over

the background transitional levels. With film-cooling (Fig.13(b)), the boundary layer is more nearly turbulent and the wake signature is lost in the turbulent heat transfer signal.

Front Pressure Surface (Build 3)

Examination of Fig. 4 shows almost no effect of coolant injection on Nusselt numbers from this row. The only discernible effect appears to be very localised and is only detectable for the first gauge downstream of the film-cooling row. This may indicate loss of the coolant into the freestream.

The schlieren photographs show coolant flowing along the blade surface for a blowing rate of 0.5, while for B.R.=1.0, lift-off appears to be happening and the trajectory of the coolant is quickly lost in the freestream. The lift-off is even more pronounced for a blowing rate of 1.5.

Figure 7 shows the effect of blowing rate on the film-cooling performance of this row with 16 bars passing. By comparison with Figure 4 it can be seen that there is very little difference produced by wake passing. This might be expected since wake passing does not trip the already turbulent boundary layer, and also the no bar results have shown that this row performance is fairly insensitive to changes in blowing rate. Thus a change in unsteady blowing rate produced by the passage of the wake will not have a significant effect. Fig. 14 shows η_{aw} for this row with wake passing. A blowing rate of 1.5 gives the highest values of η_{aw} but then falls to zero by 26 x/D. The last two experimental points have been left off this graph. This is because these points were downstream of a heater pad which was used to alter the wall temperature. Insufficient correction for the presence of this particular heater pad may have adversely affected the results.

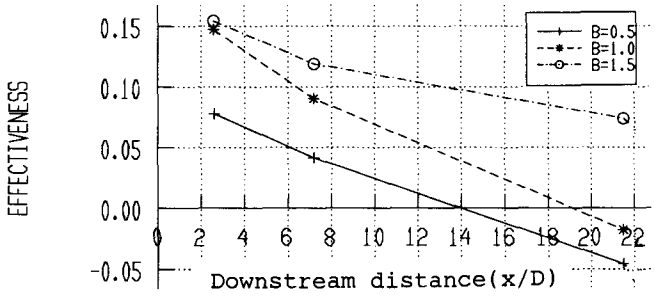

Fig. 14 Cooling effectiveness for Build 3 with 16 bar passing, at 3 blowing rates.

Rear Pressure Surface (Build 4)

The performance of this row of holes is shown in Fig. 5. Contrary to common experience with double rows of holes there is no cooling in the region downstream of injection. In fact, the levels of heat transfer are raised above the uncooled levels and so enhancement rather than cooling is produced.

Figure 15 shows η_{aw} measurements without wake passing. Here, η_{aw} is of order zero which indicates no cooling of the surface. This could be explained by lift-off of the films which are then lost in the freestream due to the curvature of the blade and the passage pressure gradient, which will carry the coolant across the passage.

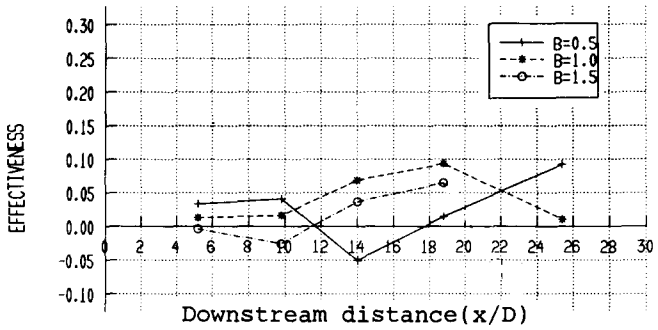

Fig. 15 Cooling effectiveness for Build 4 with no bar passing, at 3 blowing rates.

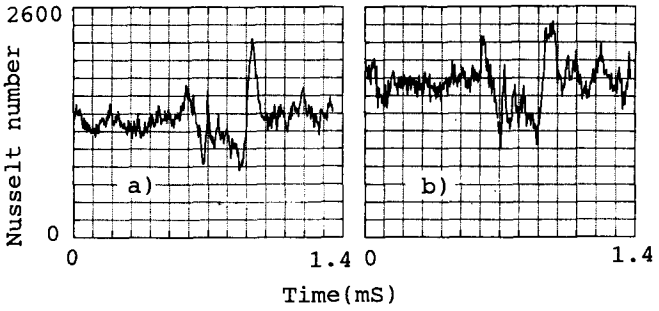

Fig. 16 Unsteady Nusselt number traces at model point 6: a) with no film cooling; b) with cooling at B.R.=1.5. 2 bars in rotating disk.

The small negative values of η_{aw} are due to scatter. Figs 16 (a) and (b) show the unsteady heat transfer traces (for MP6) for blow and no blow and show that there is no appreciable difference between the two. Measured values of film-cooling effectiveness are comparable for the two cases of bar passing and no bar passing, while the unsteady traces give the same signature for both injection present and no injection. Again, the effect of film lift-off can be seen in the η_{aw} results (Fig. 17). A blowing rate of 0.5 shows a falling value of the effectiveness with downstream distance, while for blowing rates of 1.0 and 1.5 it rises. This is because at higher blowing rates, the lifted-off film will come back to the blade surface due to blade curvature and the normal pressure gradient.

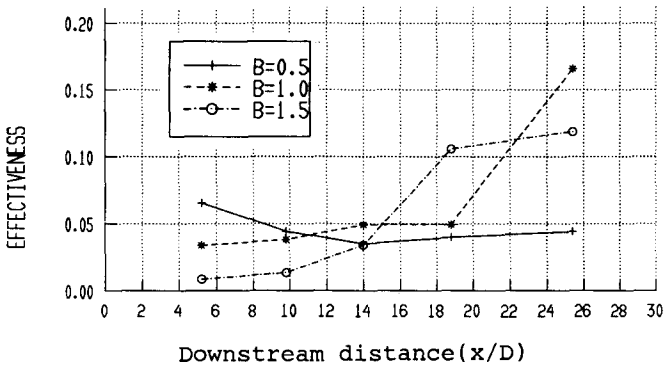

Fig. 17 Cooling effectiveness for Build 4 with 16 bar passing, at 3 blowing rates.

CONCLUSIONS

1. Heat transfer distributions have been measured for four different film-cooling configurations on a transonic turbine rotor blade both without, and with, simulated NGV wake and shock wave passing.

2. The cooling performance has been analysed using the superposition model of film-cooling together with schlieren photography flow visualisation and fast sampled heat transfer measurements.

3. The steady state cooling results show that on the suction surface an optimum blowing rate can be found. On the pressure surface, however, there is little film-cooling effect, and even enhancement of downstream heat transfer by film injection.

4. There is significant effect of NGV simulated shock wave and wake passing on the performance of the two suction surface rows. The wake enhances mixing of the film while the shock wave produces large excursions in the unsteady heat transfer rate. The unsteady shock wave signature changes when film cooling is introduced.

5. Differences in the film behaviour with wake and shock wave passing compared to the usual steady cascade heat transfer results demonstrate the importance of taking account of unsteady effects in the prediction of blade heat transfer and cooling performance.

ACKNOWLEDGEMENTS

The authors gratefully acknowledge the support of Rolls-Royce plc and the U.S. Air Force (Wright Research and Development Centre, Aero-Propulsion Laboratory, Air Force Systems Command, Wright-Patterson AFB, Ohio, Contract No. F33615-84-C-2475) for this work and the kind permission of Rolls-Royce plc to publish this paper. The work of K.J.Grindrod and J.L.Allen is also gratefully acknowledged.

REFERENCES

Choe, H., Kays, W.M., Moffat, R.J. "The Superposition Approach to Film-Cooling.", ASME Paper 74-WA/HR-27. 1974.

Doorly, D.J. and Oldfield, M.L.G., " Simulation of the Effects of Shock Wave Passing on a Turbine Rotor Blade", *J. Eng for Gas Turbines and Power*, Vol. 107, pp. 998-1006, 1985.

Dunn, M.G., Chupp, R.E., " Influence of Vane/Blade Spacing and Injection on Stage Heat-Flux Distribution" *J. Prop and Power*, Vol. 5, No.2 pp212-220 1987.

Horton, F. G. "Aerodynamics and Heat Transfer of Turbine Blading" D.Phil thesis Oxford University, 1985.

Johnson, A.B., Rigby, M.J., Oldfield, M.L.G., Ainsworth, R.W., and Oliver, M.J., " Surface Heat Transfer Fluctuations on a Turbine Rotor Blade Due to Upstream Shock Wave Passing", ASME *J. Turbomachinery*, Jan. 1989, Vol. 111, pp105-115.

Jones, T.V., Schultz, D.L., Hendley, A.D. "On the Flow in an Isentropic Light Piston Tunnel." Aero Research Council R and M No.3731. Jan.1973.

Jones, T.V. "The Superposition Model of Film Cooling and Fluid Dynamic Scaling." V.K.I. Lecture Series 1982.

Oldfield, M.L.G., Burd, H.J., and Doe, N.G., "Design of Wide-Bandwidth Analogue Circuits for Heat Transfer Instrumentation in Transient Tunnels", *Proc. 16th ICHMT Symposium on Heat and Mass Transfer in Rotating Machinery*, Dubrovnik, Hemisphere Publ. Corp., N.Y., pp. 233-258, 1984.

Rigby, M. J., Johnson, A. B., Oldfield, M.L.G., Jones, T.V., "Temperature Scaling of Turbine Blade Heat Transfer with and without Shock Wave Passing" *Proc. Ninth International Symposium on Air Breathing Engines*, Athens, Greece. Sept. 1989.

Schultz, D.L., Jones, T.V., Oldfield, M.L.G., Daniels, L.C. "A New Transient Cascade Facility for the Measurement of Heat Transfer Rates." AGARD *Conference Proceedings No. 229. High Temperature Problems in Gas Turbine Engines.* 1977.

Teekaram, A.J.H., Forth, C.J.P., Jones, T.V. "The Use of Foreign Gas to Simulate the Effects of Density Ratios in Film Cooling." ASME *J. Turbomachinery*, Jan. 1989, Vol. 111, pp57-62.